Facile Production of Biodiesel from Candlenut Oil (*Aleurites moluccana* L.) Using Photocatalytic Method by Nano Sized-ZnO Photocatalytic Agent Synthesized via Polyol Method

Hendro Juwono*, Anizun Zakiyah, Riki Subagyo, and Yuly Kusumawati

Department of Chemistry, Faculty of Science and Data Analytics, Institut Teknologi Sepuluh Nopember, Kampus ITS Keputih, Sukolilo, Surabaya 60111, Indonesia

* ***Corresponding author:***

email: hjachmad@gmail.com

Received: March 8, 2023
Accepted: August 1, 2023

DOI: 10.22146/ijc.82895

Abstract: *Biodiesel production from non-edible oil is an alternative way to reduce edible oil dependency and reduce the competition for feed and food. Candlenut oil (*Aleurites moluccana *L.) is one of the non-edible oils which can be used as feedstock for biodiesel production since they have a high oil content. Herein, the biodiesel production from candlenut oil has been conducted using zinc oxide (ZnO) synthesized by the polyol method. Polyol methods facilitated the formation of ZnO nanoparticles with various shapes, including spherical, rod, and hexagonal. Besides, ZnO showed a mesoporous characteristic, facilitating the conversion of fat fatty acid to fatty acid methyl ester (FAME) of 61%. Increasing ZnO dosage led to enhancing the FAME yield. Similarly, the FAME yield was also improved by increasing the reaction time. The results of esterification of candlenut oil and methanol yielded 70.76% FAME with 2% nano-ZnO polyol catalyst at 180 min reaction time at room temperature whilst being stirred constantly at 400 rpm. A good FAME conversion using ZnO at room temperature provides good information to produce biodiesel with a simple method. Apart from that, photocatalytic promoted transesterification at room temperature, which is beneficial for reducing energy consumption.*

Keywords: *biodiesel; esterification; candlenut oil; ZnO nanoparticle; polyol technique*

■ INTRODUCTION

The development of renewable energy has been investigated in order to meet the energy demand. Biodiesel is an alternative fuel among various renewable energy which non-toxic, biodegradable, and environmentally friendly [1-2]. As reviewed by Tabatabaei et al. [3], various method has been developed to yield biodiesel, including direct use and blending, microemulsion, pyrolysis, and transesterification. Direct use and blending showed a high viscosity and free fatty acid due to the incomplete reaction, even though this method offered a low-cost production. Microemulsion methods facilitated biodiesel production with lower viscosity and higher liquidity. However, the obtained biodiesel using the microemulsion method has a heavy deposition of carbon and inadequate combustion. Pyrolysis exhibited satisfactory physical and chemical properties of the yielded biodiesel. Nevertheless, the production cost of pyrolysis is very high. The transesterification method is a common method for biodiesel production. The transesterification method is carried out at 60–70 °C to convert the oils and fats into biodiesel in the presence of a suitable catalyst [4-5]. Besides, biodiesel production via transesterification methods can be conducted using various types of feedstocks that contain free fatty acids and/or triglycerides [6]. Various edible oil was used for biodiesel production, including canola oil [7-8], rapeseed oil [9], peanut oil [10], sunflower oil [11-12], coconut oil [13], palm oil [14-15], and safflower oil [16]. However, utilizing edible sources for biodiesel production led to ecological imbalances and deforestation. Therefore, non-edible oil can be used as an alternative feedstock for biodiesel production. The usage of non-edible oil decreases the edible oil

dependency and reduces the competition for feed and food [17]. Various non-edible oils have been successfully converted into biodiesel, including jatropha oil [18], karanja oil [19], mahua oil [20], and moringa oil [21]. Among all the potential non-edible oil, candlenut oil is a potentially new feedstock for biodiesel generation. Candlenut (*Aleurites moluccana* L.) is a type of plant that contains a fairly high oil content, approximately 55–65% oil in its seeds. Candlenut oil is flammable making it able to be used as a fuel. Previous research has shown that *A. moluccana* could produce biodiesel with superior properties when combined with an ester content of more than 99% [22]. Generally, biodiesel production via an esterification reaction is carried out using a homogeneous catalyst such as sulfuric acid [23-24], potassium hydroxide [25], and sodium hydroxide [26]. However, the use of homogeneous catalysts still has several disadvantages, such as being less economical since they are only used once and require a lot of solvents to wash the reaction products [27]. Therefore, using heterogeneous catalysts can be an alternative to overcome these problems.

Photocatalytic-assisted transesterification has been developed to generate biodiesel. Photocatalytic-assisted transesterification was carried out at room temperature, which is beneficial to reduce energy consumption since the transesterification process was normally done at various temperatures. Previously, Corro et al. [28] developed photocatalytic-assisted transesterification to yield biodiesel from waste frying oil. They combined chromium (Cr) and silica (SiO_2) as a heterogeneous photocatalyst to produce biodiesel. Interestingly, the addition of Cr on SiO_2 facilitated the photoreaction to yield the biodiesel with a fatty acid methyl ester (FAME) percentage of ~98%. TiO_2 has also been reported for biodiesel production via a photocatalytic process. As reported by Ambrosio et al. [29], FAME percentages were achieved at 95% using TiO_2/H_2O_2 system under Hg lamp vapor irradiation.

Apart from that, zinc oxide (ZnO) was also developed for biodiesel production [4,30]. ZnO has a strong acid site which makes this oxide being able to be applied as a catalyst in reactions that require acidic properties, such as esterification reactions to produce biodiesel, which composed of FAME [31]. The strong Lewis acid of ZnO was generated by the appearance of Zn^{2+} at the outermost layer of the ZnO surface [32]. In addition, ZnO can easily form nano-sized particle, which plays a crucial role and resolve various bottleneck problems associated with the esterification process in biodiesel production. The nano-sized ZnO also increases the selectivity and catalytic activity [33]. Due to its hexagonal wurtzite nature, nano-sized ZnO also possesses a higher affinity and oxygen vacancy [34-35].

Various methods have been used to obtain nano-sized ZnO, including coprecipitation [36], hydrothermal [37], solvothermal [38], solid-state [39], electrochemical [40], and precursor thermal decomposition [41]. However, the mentioned synthesis methods have disadvantages to the synthesis of nano-sized ZnO. Coprecipitation requires a stabilizer and needs post-treatment to remove the impurities. Hydrothermal and solvothermal require autoclave reactors and are challenging to control the size of ZnO. Solid-state is a simple method to synthesize ZnO. However, this process must be carried out several times in order to yield a nanoparticle of ZnO. The electrochemical method is very suitable for generating ZnO with controlled size and morphology. However, the equipment for the electrochemical process is expensive. Thermal deposition is an excellent method to prepare a high purity of nano-ZnO. Despite its advantages, the equipment is very expensive, and the source material may be limited. In order to overcome the disadvantages, the polyol method has been designed to generate a nano-sized ZnO. The polyol technique is a nanoparticle synthesis method that utilizes different types of diols as reaction media [42]. Polyols also act as stabilizing agents and regulate particle growth. This method has many advantages due to the process being easy, simple, and flexible. Furthermore, the polyol technique offers the ability to form nanoparticles directly, does not require a calcination process, and the growth of nanoparticles can be controlled both in shape and size [43].

As proposed in this work, the production of biodiesel has been done at room temperature using

nano-sized ZnO. ZnO was prepared by polyol methods. The polyol methods facilitated the formation of nano-sized ZnO. In addition, polyol methods also promoted the formation of mesoporous ZnO, which is very advantageous to attach the precursor to obtain biodiesel. The optimization of photocatalyst dosage and reaction time were investigated to provide the optimum condition for biodiesel production using ZnO at room temperature.

■ EXPERIMENTAL SECTION

Materials

The materials used in this study were sodium hydroxide (NaOH, Sigma-Aldrich, 99%), zinc acetate dihydrate ($Zn(CH_3COO)_2{\cdot}H_2O$, Sigma-Aldrich, 99.5%), diethylene glycol (DEG, Sigma-Aldrich, 99%), ethanol (EtOH, Full time, 96%), acetone (Full time, 99%), methanol (Merck, 99%), and demineralized water. The candlenut oil was bought from SIPA, Sidoarjo, Indonesia.

Instrumentation

In this study, several instruments were used to investigate the properties of ZnO. The crystallinity and structural phase of the synthesized ZnO nanocatalyst was verified through X-ray diffraction (XRD, Philips PW1140/90) with Cu-Kα radiation (λ) of 0.15406 nm and 0–80° scanning angle range at room temperature. The surface morphologies and the particle sizes were analyzed through the field emission scanning electron microscope (FESEM, Themo Scientific Quattro S) and transmission electron microscope (TEM Hitachi HT7700). The total surface area and the pore size distributions were measured using the nitrogen (N_2) physisorption (Quantachrome Nova 4200e) at 77 K using the NLDFT analysis method with a degassing temperature of 120 °C for 8 h. The resulted photo-transesterification was analyzed using Gas chromatography-mass spectrometry (GC-MS, Agilent Technologies 7890A GC-5975MS)

Procedure

Synthesis of ZnO nanocatalyst

ZnO nanoparticles were synthesized by polyol technique using a reflux system as shown in Fig. 1(a), the same technique used in the previous study carried out by Hosni et al. [42]. The concentration of Zn^{2+} (z) was 0.5 mol L^{-1}, the ratio of H_2O:Zn^{2+} concentration (h) was 5:1, and the ratio of NaOH:Zn^{2+} (b) was 1:1. The synthesis mixture was prepared by dissolving 21.95 g of $Zn(CH_3COO)_2{\cdot}H_2O$, 4 g of NaOH, and 5.4 mL of demineralized water in 194.6 mL of DEG. The mixture was subsequently refluxed for 2 h at 161 °C whilst being stirred at 600 rpm until a white mixture was obtained. The mixture was then centrifuged at 10,000 rpm for 5 min in order to separate the white suspension from the solvent. Next, the white suspension obtained was washed several times with EtOH (Full time, 96%) and acetone (Full time, 99%). Subsequently, the product was dried at 80 °C for 48 h until the white powder was obtained.

Esterification of candlenut oil

The esterification reaction of candlenut oil was carried out with a ratio of oil to methanol of 1:3. Initially, 100 g (108.13 mL) of candlenut oil and 43.25 mL of methanol were prepared in a batch reactor as depicted in Fig. 1(b). Thereafter, the various amounts of ZnO nanocatalyst were added and the running times were started. The reactions were carried out for 60, 120, and 180 min with continuous stirring at 400 rpm. During the reaction, the UV-LED lamp was turned on to drive the photocatalytic reaction. After the reaction times had finished, each phase of the mixture was separated using a centrifuge at 10,000 rpm for 5 min. The mixture was separated into three phases, the upper phase was the excess of the methanol, the middle phase was the main product, and the lower phase was the catalyst. Subsequently, the composition of the main product was further analyzed with GC-MS.

■ RESULTS AND DISCUSSION

Morphologies and Properties of ZnO

The phase structure, crystallinity, and pore properties of the ZnO catalyst were synthesized using the polyol technique, as illustrated in Fig. 1. The XRD results in Fig. 2(a) signified that the synthesized ZnO had similar characteristic peaks with a standard ZnO (JCPDS No. 36-1451), indicating that the synthesized ZnO had a hexagonal (wurtzite) structure. The characteristic peaks of ZnO synthesized by the polyol technique were observed

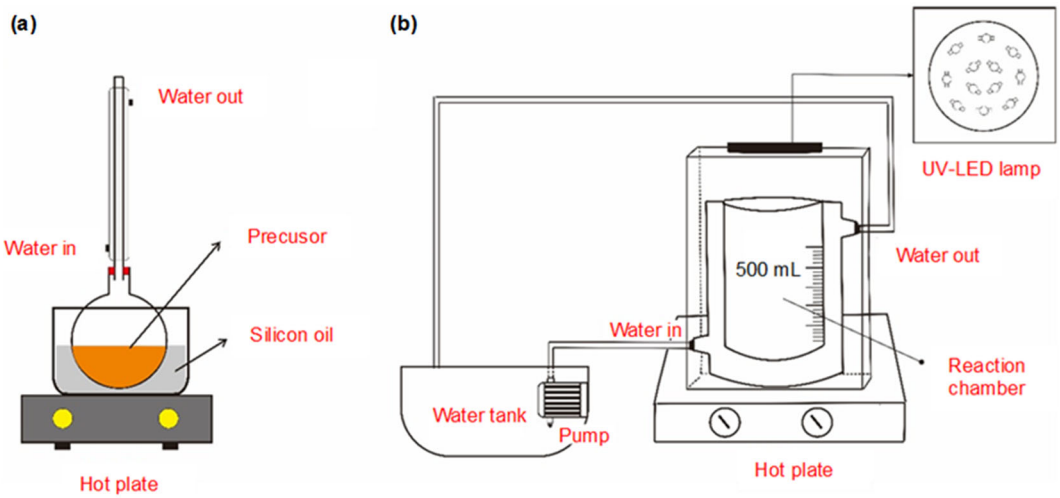

Fig 1. (a) Reflux system for polyol method and (b) batch photocatalytic reactor for biodiesel production

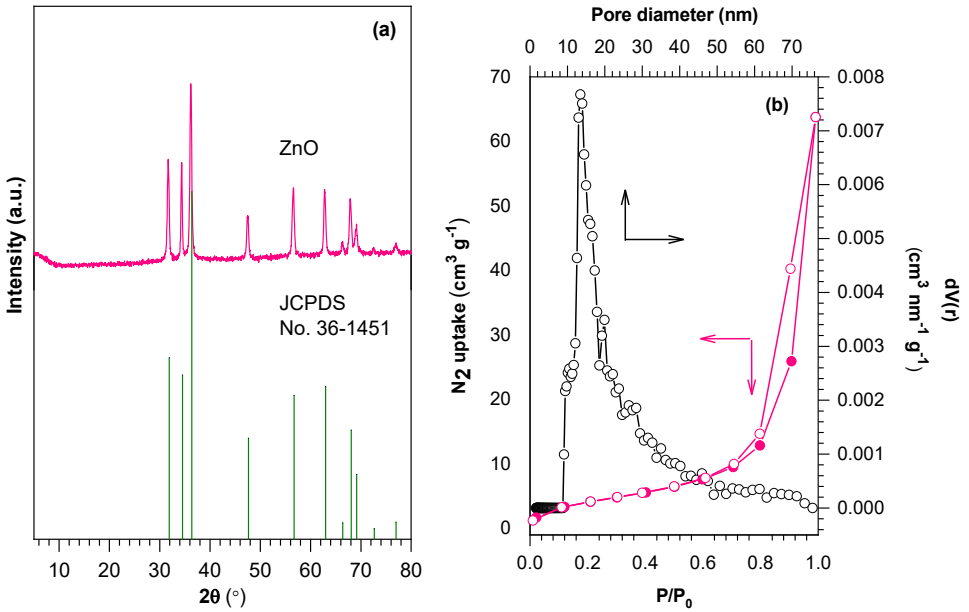

Fig 2. (a) XRD pattern of ZnO, (b) N_2 adsorption-desorption and pore size diameter of ZnO

at 2θ = 31.67°, 34.40°, and 36.17° associated with the (100), (002), and (101) plane, which is in line with previous studies [36,44] using coprecipitation methods and gelatine templates, respectively. The sharp peaks with high intensity hinted that the synthesized ZnO had a crystalline structure without any post-synthesis heat treatment. In addition, the absence of impurities was observed, indicating that the polyol method promotes the formation of ZnO with good purity. The intensity of (101) peak is higher compared to other peaks, revealing that ZnO grows to the (101) direction [45]. Additionally, those peaks are shifted approximately 0.08° compared to the JCPDS standard, indicating the enhancement of interplanar spacing due to the formation of oxygen vacancy [46]. This result is in agreement with the previous study by Bi et al. [47], showing that the formation of oxygen vacancy enhances the interplanar spacing and results in the decrease of (101) diffraction angle.

The porosity of the synthesized ZnO nanocatalyst was investigated using the N_2 adsorption-desorption isotherm. The surface area and pore size distribution were also calculated by implementing the NLDFT

calculation method, and the results are shown in Fig. 2(b). The total surface area of the synthesized ZnO is 15.5 $m^2 g^{-1}$. The prepared ZnO shows a low amount of N_2 adsorption at P/P_0 of 0–0.7 and subsequently enhanced until P/P_0 of 0.99. The obtained isotherm signifies a type IV isotherm according to IUPAC recommendation, revealing that the prepared ZnO is a mesoporous material [44]. The hysteresis loop is also generated in ZnO due to the condensation process during the desorption process [48]. The yielded hysteresis loop in ZnO is associated with H3-type hysteresis, corresponding to interconnected mesopores with non-uniform shape and size [49], which is confirmed by FESEM and TEM analysis. The type of hysteresis demonstrates the mesopores materials with agglomerate or aggregates characteristic of nanoparticles forming slit-shaped pores with non-uniform size and shape [50]. The hysteresis loop at P/P_0 ~0.85–0.99 indicates the formation of interparticle voids caused by textural porosity between the particles [51]. Based on the pore size distribution calculation, it is exhibited that the pore sizes of synthesized ZnO are mostly around 12 nm.

FESEM and TEM are shown in Fig. 3. Based on the FESEM result in Fig. 3(a), the polyol technique used in this study has successfully produced ZnO with nanoparticle sizes. The ZnO nanoparticles agglomerate and generate a big particle size in micrometer. This result is in line with the previous study by Mahamuni et al. [52] that reported the agglomeration of nanoparticle ZnO synthesized by the polyol method. In order to obtain better imaging information in relation to the size and shape of the synthesized ZnO nanoparticles, TEM analysis was carried out, as depicted in Fig. 3(b). In terms of the shapes of the particles, they are relatively hexagonal, rod, and spherical. The particle size of ZnO is confirmed using particle size distribution by estimating 100 individual particles of the projected area in the TEM images, as shown in Fig. 4. The average diameter size of ZnO is found in the range of 10–210 nm. The average diameter of 20–80 nm shows a high frequency of ZnO, indicating that most of the synthesized ZnO size is under 100 nm. Compared to the previous study by Chieng and Loo [53], the obtained ZnO has a similar size (under 100 nm) which confirmed that the polyol method can promote the generation of nano-sized ZnO.

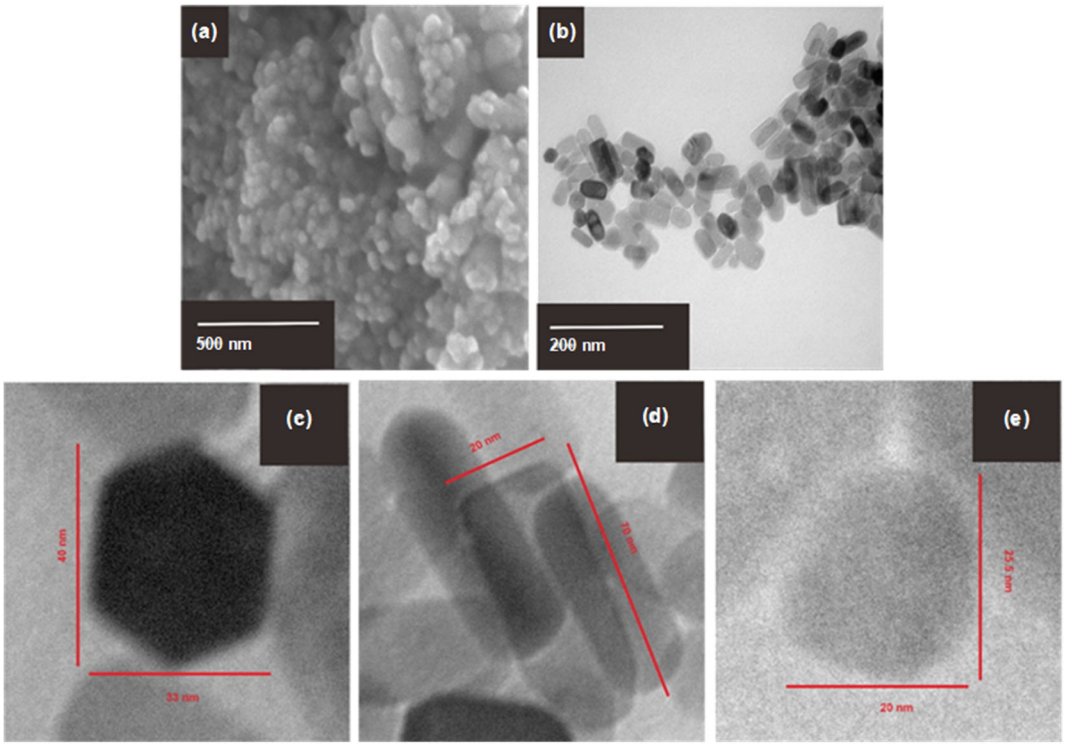

Fig 3. (a) FESEM, (b) TEM images of ZnO, and the (c) hexagonal, (d) rods and (e) sphere morphology of ZnO

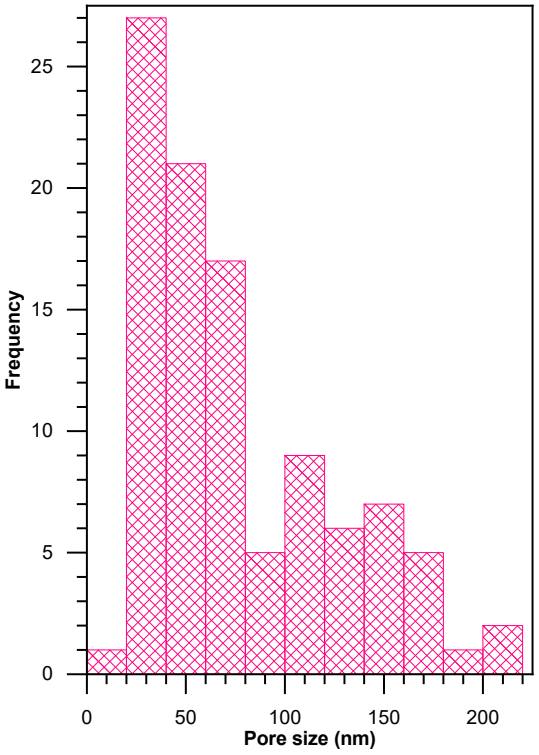

Fig 4. Pore size distribution of ZnO

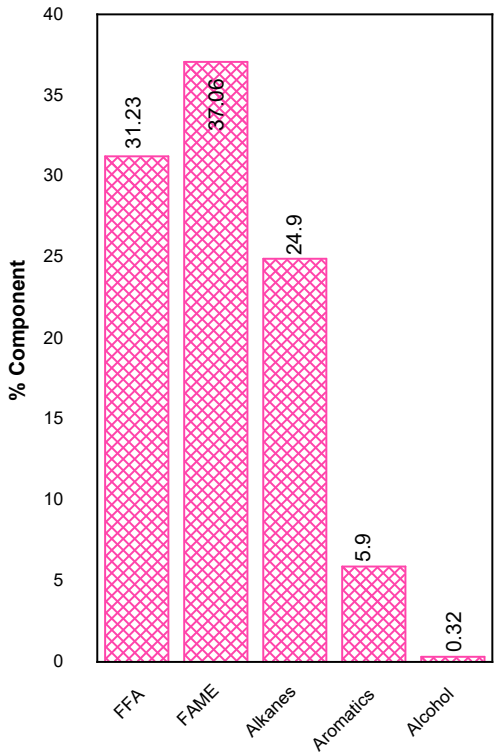

Fig 5. Component of candlenut oil

Photo Esterification of Candlenut Oil

Fig. 5 shows the components of candlenut oil used in this study. The main components were FFA, FAME, and alkanes compounds. Candlenut oil also contains a small number of aromatic compounds and alcohol. The GC-MS results showed that the candlenut oil contained a high amount of FFA of approximately 31.23%. The main FFA compounds in the candlenut oil were linoleic acid (9(*Z*),12(*Z*)-octadecadienoic acid) and palmitic acid (*n*-hexadecanoic acid). The candlenut oil itself initially contains approximately 37.06% FAME compounds. In this study, the FFA content of candlenut oil was converted into FAME compounds through an esterification reaction with methanol and ZnO polyol nanocatalyst.

Fig. 6(a) displays the effects of ZnO polyol nanocatalyst amount (%w/w ZnO/candlenut oil) to the FAME percentage results for 180 min esterification time with an oil: methanol ratio of 1:3 at room temperature whilst being stirred at 400 rpm. The results signified that the addition of ZnO polyol nanocatalyst to the reaction was able to increase the FAME yield. The plot also revealed that the amount of FAME percentage increased with increasing the amount of ZnO polyol nanocatalyst (0.5, 1.5, and 2.0%). Increasing the amount of ZnO led to enhancing the active surface for the photo-transesterification process. Consequently, the amount of generated FAME is increased [54]. An optimum FAME yield can be obtained after adding 2.0% of ZnO polyol nano catalyst to the reaction, with FAME percentage result obtained is approximately 70.76%. This result also demonstrated that the synthesized ZnO nano through the polyol method was successfully performed as a catalyst to convert FFA into FAME in the esterification reaction of candlenut oil. However, the percentage of FAME is slightly reduced compared to the previous study by Zhang et al. [55], reporting that the FAME conversion from waste cooking soybean oil was 100% using graphitic carbon nitride supported molybdenum catalyst. This result is very reasonable since only ZnO is used as a photocatalyst, yielding a fast recombination process compared to modified photocatalysts [56]. As a result, the transesterification process promoted by the photo-redox reaction is low compared to modified photocatalysts.

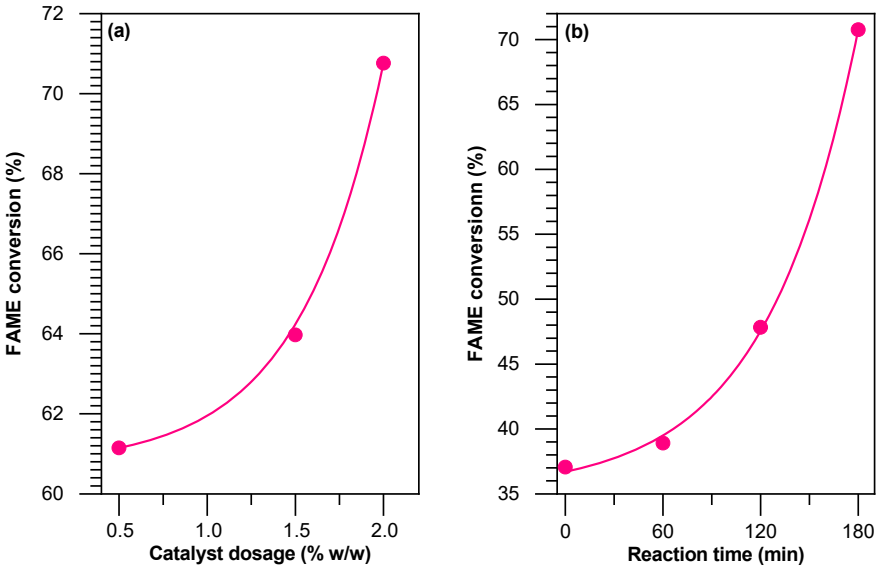

Fig 6. (a) Effect of catalyst dosage (b) Effect of esterification time

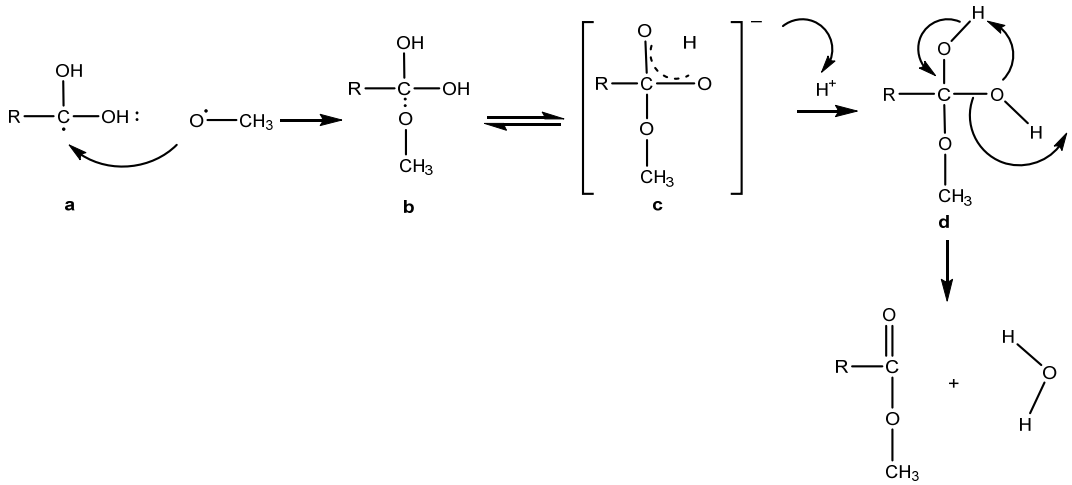

Fig 7. Proposed mechanism of oil and methanol photo-esterification through ZnO catalyst

Fig. 6(b) displays the effects of esterification time (60, 120, and 180 min) with respect to the FAME percentage result in the presence of 2.0% ZnO polyol nanocatalyst with oil: methanol ratio of 1:3 at room temperature whilst being stirred at 400 rpm. The result hinted that the reaction time highly affected the FAME percentage result. A small increase in FAME percentage was obtained after the reagent was being reacted for 60 min. Increasing the reaction time significantly increased the FAME percentage result, which was around 47% and 70% for 120 and 180 min reaction time, respectively. It can be seen that increasing the time temperature enhanced the time of the transesterification reaction via the photocatalysis process. According to the process, the photocatalytic process promotes the transesterification process to yield biodiesel. During the UV light irradiation, electrons on the valence band (VB) of ZnO were excited to the conduction band of ZnO. At the time, holes were also generated on the VB of ZnO. The electrons would react with the FFA molecule to form a radical compound of FFA (compound **a**) [28]. Besides, holes would react with methanol to form methanol radicals and protons. Methanol radical would react with FFA methanol to form compound **b**, followed by attacking H^+ to yield compound **c**. Since the oxygen atom has a lone pair electron, it is possible to attack the

hydrogen atom of a hydroxyl group in compound **d**, which has the lowest electronegativity. Thus, the oxygen atom of the hydroxyl group reacted with the hydrogen atom of another hydroxyl group and yielded a water molecule and methyl ester group, as illustrated in Fig. 7.

■ CONCLUSION

The production of biodiesel from candlenut oil using ZnO via photocatalytic-assisted transesterification has been successfully carried out. ZnO was prepared via the polyol method and exhibited a nanoparticle size of 20–200 nm and a surface area of 15.5 $m^2 g^{-1}$. The pore size distribution of ZnO was mostly around 10–20 nm. Besides, various morphologies were generated by polyol methods, including spherical, rods, and hexagonal. The GC-MS result reported that the application of the candlenut oil esterification reaction was successfully carried out. The FFA content in candlenut oil has been converted into FAME with the assistance of nano-ZnO polyol as the catalyst. The effect of ZnO percentage and esterification time revealed that the FAME percentage increased either along with the increasing ZnO percentage (0.5, 1.5, and 2.0% w/w) or with the increasing reaction time (0, 60, 120, and 180 min). The yield of FAME percentage was approximately 70.76%, which was obtained in the reaction using 2.0% nano-ZnO polyol under 180 min reaction time at room temperature whilst being stirred constantly at 400 rpm. The photocatalytic process promotes the transesterification process at room temperature, which is beneficial for reducing energy consumption. Apart from that, a moderate FAME percentage is obtained due to the limitation of ZnO in charge carrier transfer and separation as a single photocatalyst.

■ ACKNOWLEDGMENTS

The authors gratefully thank the Deputy for Research and Development, Ministry of Research and Technology of the Republic of Indonesia for funding this research through the Fundamental Research Scheme with contract number 1510/PKS/ITS/2022.

■ REFERENCES

[1] Maleki, B., and Talesh, S.S.A., 2022, Optimization of ZnO incorporation to αFe_2O_3 nanoparticles as an efficient catalyst for biodiesel production in a sonoreactor: Application on the CI engine, *Renewable Energy*, 182, 43–59.

[2] Abukhadra, M.R., Ibrahim, S.M, Yakout, S.M., El-Zaidy, M.E., and Abdeltawab, A.A., 2019, Synthesis of Na^+ trapped bentonite/zeolite-P composite as a novel catalyst for effective production of biodiesel from palm oil: Effect of ultrasonic irradiation and mechanism, *Energy Convers. Manage.*, 196, 739–750.

[3] Tabatabaei, M., Aghbashlo, M., Dehhaghi, M., Panahi, H.K.S., Mollahosseini, A., Hosseini, M., and Soufiyan, M.M., 2019, Reactor technologies for biodiesel production and processing: A review, *Prog. Energy Combust. Sci.*, 74, 239–303.

[4] Rao, A.V.R.K., Dudhe, P., and Chelvam, V., 2021, Role of oxygen defects in basicity of Se doped ZnO nanocatalyst for enhanced triglyceride transesterification in biodiesel production, *Catal. Commun.*, 149, 106258.

[5] Avhad, M.R., and Marchetti, J.M., 2016, Innovation in solid heterogeneous catalysis for the generation of economically viable and ecofriendly biodiesel: A review, *Catal. Rev.: Sci. Eng.*, 58 (2), 157–208.

[6] Hoekman, S.K., Broch, A., Robbins, C., Ceniceros, E., and Natarajan, M., 2012, Review of biodiesel composition, properties, and specifications, *Renewable Sustainable Energy Rev.*, 16 (1), 143–169.

[7] Khatibi, M., Khorasheh, F., and Larimi, A., 2021, Biodiesel production via transesterification of canola oil in the presence of Na–K doped CaO derived from calcined eggshell, *Renewable Energy*, 163, 1626–1636.

[8] Murguía-Ortiz, D., Cordova, I., Manriquez, M.E., Ortiz-Islas, E., Cabrera-Sierra, R., Contreras, J.L., Alcántar-Vázquez, B., Trejo-Rubio, M., Vázquez-Rodríguez, J.T., and Castro, L.V., 2021, Na-CaO/MgO dolomites used as heterogeneous catalysts in canola oil transesterification for biodiesel production, *Mater. Lett.*, 291, 129587.

[9] Fallah Kelarijani, A., Gholipour Zanjani, N., and Kamran Pirzaman, A., 2020, Ultrasonic assisted transesterification of rapeseed oil to biodiesel using

nano magnetic catalysts, *Waste Biomass Valorization*, 11 (6), 2613–2621.

[10] Jung, S., Kim, M., Jeon, Y.J., Tsang, Y.F., Bhatnagar, A., and Kwon, E.E., 2021, Valorization of aflatoxin contaminated peanut into biodiesel through non-catalytic transesterification, *J. Hazard. Mater.*, 416, 125845.

[11] Salmasi, M.S., Kazemeini, M., and Sadjadi, S., 2020, Transesterification of sunflower oil to biodiesel fuel utilizing a novel K_2CO_3/Talc catalyst: Process optimization and kinetics investigations, *Ind. Crops Prod.*, 156, 112846.

[12] Lima, A.C., Hachemane, K., Ribeiro, A.E., Queiroz, A., Gomes, M.C.S., and Brito, P., 2022, Evaluation and kinetic study of alkaline ionic liquid for biodiesel production through transesterification of sunflower oil, *Fuel*, 324, 124586.

[13] Ahmad, A.A., Zulkurnain, N., Mat Rosid, S.J., Azid, A., Endut, A., Toemen, S., Ismail, S., Wan Abdullah, W.N., Aziz, S.M., Mohammed Yusoff, N., Mat Rosid, S., and Nasir, N.A., 2022, Catalytic transesterification of coconut oil in biodiesel production: A review, *Catal. Surv. Asia*, 26 (3), 129–143.

[14] Qu, T., Niu, S., Zhang, X., Han, K., and Lu, C., 2021, Preparation of calcium modified Zn-Ce/Al_2O_3 heterogeneous catalyst for biodiesel production through transesterification of palm oil with methanol optimized by response surface methodology, *Fuel*, 284, 118986.

[15] Woranuch, W., Ngaosuwan, K., Kiatkittipong, W., Wongsawaeng, D., Appamana, W., Powell, J., Lalthazuala Rokhum, S., and Assabumrungrat, S., 2022, Fine-tuned fabrication parameters of CaO catalyst pellets for transesterification of palm oil to biodiesel, *Fuel*, 323, 124356.

[16] Nogales-Degaldo, S., Encinar, J.M., and González Cortés, Á., 2021, High oleic safflower oil as a feedstock for stable biodiesel and biolubricant production, *Ind. Crop Prod.*, 170, 113701.

[17] Mathew, G.M., Raina, D., Narisetty, V., Kumar, V., Saran, S., Pugazhendi, A., Sindhu, R., Pandey, A., and Binod, P., 2021, Recent advances in biodiesel production: Challenges and solutions, *Sci. Total Environ.*, 794, 148751.

[18] Athar, M., Imdad, S., Zaidi, S., Yusuf, M., Kamyab, H., Jaromír Klemeš, J., and Chelliapan, S., 2022, Biodiesel production by single-step acid-catalysed transesterification of jatropha oil under microwave heating with modelling and optimisation using response surface methodology, *Fuel*, 322, 124205.

[19] Kumar, R., and Pal, P., 2021, Lipase immobilized graphene oxide biocatalyst assisted enzymatic transesterification of *Pongamia pinnata* (karanja) oil and downstream enrichment of biodiesel by solar-driven direct contact membrane distillation followed by ultrafiltration, *Fuel Process. Technol.*, 211, 106577.

[20] Gandhi, S.S., and Gogate, P.R., 2021, Process intensification of fatty acid ester production using esterification followed by transesterification of high acid value mahua (*Iluppai ennai*) oil: Comparison of the ultrasonic reactors, *Fuel*, 294, 120560.

[21] Rashid, U., Anwar, F., Ashraf, M., Saleem, M., and Yusup, S., 2011, Application of response surface methodology for optimizing transesterification of *Moringa oleifera* oil: Biodiesel production, *Energy Convers. Manage.*, 52 (8-9), 3034–3042.

[22] de O Lima, J.R., Gasparini, F., Camargo, N.D.L., Ghani, Y.A., da Silva, R.B., and de Oliveira, J.E., 2011, Indian-nut (*Aleurites moluccana*) and tucum (*Astrocaryum vulgare*), non agricultural sources for biodiesel production using ethanol composition, characterization and optimization of the reactional production conditions, *World Renewable Energy Congress – Sweden*, 8-13 May 2011, Linköping, Sweden, 109–116.

[23] Juwono, H., Triyono, T., Sutarno, S., Wahyuni, E.T., Ulfin, I., and Kurniawan, F., 2017, Production of biodiesel from seed oil of nyamplung (*Calophyllum inophyllum*) by Al-MCM-41 and its performance in diesel engine, *Indones. J. Chem.*, 17 (2), 316–321.

[24] Redjeki, A.S., Sukirno, S., and Slamet, S., 2019, Photocatalytic esterification process for methyl

ester synthesis from kemiri sunan oil: A novel approach, *AIP Conf. Proc.*, 2085 (1), 020058.

[25] Rahman, M.A., Aziz, M.A., Al-khulaidim, R.A., Sakib, N., and Islam, M., 2017, Biodiesel production from microalgae *Spirulina maxima* by two step process: Optimization of process variable, *J. Radiat. Res. Appl. Sci.*, 10 (2), 140–147.

[26] Zhang, Y., and You, H., 2015, Study on biodiesel production from rapeseed oil through the orthogonal method, *Energy Sources, Part A*, 37 (4), 422–427.

[27] Al-Saadi, A., Mathan, B., and He, Y., 2020, Esterification and transesterification over SrO–ZnO/Al_2O_3 as a novel bifunctional catalyst for biodiesel production, *Renewable Energy*, 158, 388–399.

[28] Corro, G., Sánchez, N., Pal, U., Cebada, S., and Fierro, J.L.G., 2017, Solar-irradiation driven biodiesel production using Cr/SiO_2 photocatalyst exploiting cooperative interaction between Cr^{6+} and Cr^{3+} moieties, *Appl. Catal., B*, 203, 43–52.

[29] Ambrosio, E., Lucca, D.L., Garcia, M.H.B., de Souza, M.T.F., de S. Freitas, T.K.F., de Souza, R.P., Visentainer, J.V., and Garcia, J.C., 2017, Optimization of photocatalytic degradation of biodiesel using TiO_2/H_2O_2 by experimental design, *Sci. Total Environ.*, 581-582, 1–9.

[30] Wang, A., Quan, W., Zhang, H., Li, H., and Yang, S., 2021, Heterogeneous ZnO-containing catalysts for efficient biodiesel production, *RSC Adv.*, 11 (33), 20465–20478.

[31] Bancquart, S., Vanhove, C., Pouilloux, Y., and Barrault, J., 2001, Glycerol transesterification with methyl stearate over solid basic catalysts: I. Relationship between activity and basicity, *Appl. Catal., A*, 218 (1-2), 1–11.

[32] Kothandapani, J., Ganesan, A., Mani, G.K., Kulandaisamy, A.J., Rayappan, J.B.B., and Selva Ganesan, S., 2016, Zinc oxide surface: A versatile nanoplatform for solvent-free synthesis of diverse isatin derivatives, *Tetrahedron Lett.*, 57 (31), 3472–3475.

[33] Baskar, G., and Aiswarya, R., 2016, Trends in catalytic production of biodiesel from various feedstocks, *Renewable Sustainable Energy Rev.*, 57, 496–504.

[34] Yuan, H., Xu, M., and Huang, Q.Z., 2014, Effects of pH of the precursor sol on structural and optical properties of Cu-doped ZnO thin films, *J. Alloys Compd.*, 616, 401–407.

[35] Dantas, J., Leal, E., Mapossa, A.B., Cornejo, D.R., and Costa, A.C.F.M., 2017, Magnetic nanocatalysts of $Ni_{0.5}Zn_{0.5}Fe_2O_4$ doped with Cu and performance evaluation in transesterification reaction for biodiesel production, *Fuel*, 191, 463–471.

[36] Subagyo, R., Kusumawati, Y., and Widayatno, W.B., 2020, Kinetic study of methylene blue photocatalytic decolorization using zinc oxide under UV-LED irradiation, *AIP Conf. Proc.*, 2237, 02001.

[37] Sun, X.M., Chen, X., Deng, Z.X., and Li, Y.D., 2003, A CTAB-assisted hydrothermal orientation growth of ZnO nanorods, *Mater. Chem. Phys.*, 78 (1), 99–104.

[38] Guo, L., Ji, Y.L., Xu, H., Simon, P., and Wu, Z., 2002, Regularly shaped, single-crystalline ZnO nanorods with wurtzite structure, *J. Am. Chem. Soc.*, 124 (50), 14864–14865.

[39] Wang, Z., Zhang, H., Zhang, L., Yuan, J., Yan, S., and Wang, C., 2003, Low-temperature synthesis of ZnO nanoparticles by solid-state pyrolytic, *Nanotechnology*, 14 (1), 11.

[40] Khaleel, R.S., and Hashim, M.S., 2020, Fabrication of ZnO sensor to measure pressure, humidity and sense vapors at room temperature using the rapid breakdown anodization method, *Kuwait J. Sci.*, 47, 42–49.

[41] Pillai, S.C., Kelly, J.M., McCormack, D.E., O'Brien, P., and Ramesh, R., 2003, The effect of processing conditions on varistors prepared from nanocrystalline ZnO, *J. Mater. Chem.*, 13 (10), 2586–2590.

[42] Hosni, M., Kusumawati, Y., Farhat, S., Jouini, N., and Pauporté, T., 2014, Effects of oxide nanoparticle size and shape on electronic structure, charge transport, and recombination in dye-

sensitized solar cell photoelectrodes, *J. Phys. Chem. C*, 118 (30), 16791–16798.

[43] Dong, H., Chen, Y.C., and Feldmann, C., 2015, Polyol synthesis of nanoparticles: Status and options regarding metals, oxides, chalcogenides, and non-metal elements, *Green Chem.*, 17 (8), 4107–4132.

[44] Prasetyoko, D., Sholeha, N.A., Subagyo, R., Ulfa, M., Bahruji, H., Holilah, H., Pradipta, M.F., and Jalil, A.A., 2023, Mesoporous ZnO nanoparticles using gelatin - Pluronic F127 as a double colloidal system for methylene blue photodegradation, *Korean J. Chem. Eng.*, 40 (1), 112–123.

[45] Das, A., and Nair, R.G., 2020, Effect of aspect ratio on photocatalytic performance of hexagonal ZnO nanorods, *J. Alloys Compd.*, 817, 153277.

[46] Bi, X., Du, G., Kalam, A., Sun, G., Yu, Y., Su, Q., Xu, B., and Al-Sehemi, A.G., 2021, Tuning oxygen vacancy content in TiO_2 nanoparticles to enhance the photocatalytic performance, *Chem. Eng. Sci.*, 234, 116440.

[47] Bi, T., Du, Z., Chen, S., He, H., Shen, X., and Fu, Y., 2023, Preparation of flower-like ZnO photocatalyst with oxygen vacancy to enhance the photocatalytic degradation of methyl orange, *Appl. Surf. Sci.*, 614, 156240.

[48] Subagyo, R., Tehubijuluw, H., Utomo, W.P., Rizqi, H.D., Kusumawati, Y., Bahruji, H., and Prasetyoko, D., 2022, Converting red mud wastes into mesoporous ZSM-5 decorated with TiO_2 as an eco-friendly and efficient adsorbent-photocatalyst for dyes removal, *Arabian J. Chem.*, 15 (5), 103754.

[49] Liu, Y., She, N., Zhao, J., Peng, T., and Liu, C., 2013, Fabrication of hierarchical porous ZnO and its performance in Ni/ZnO reactive-adsorption desulfurization, *Pet. Sci.*, 10 (4), 589–595.

[50] Santos, R.M.M., Tronto, J., Briois, V., and Santilli, C.V., 2017, Thermal decomposition and recovery properties of ZnAl-CO_3 layered double hydroxide for anionic dye adsorption: Insight into the aggregative nucleation and growth mechanism of the LDH memory effect, *J. Mater. Chem. A*, 5 (20), 9998–10009.

[51] A'yuni, Q., Rahmayanti, A., Hartati, H., Purkan, P., Subagyo, R., Rohmah, N., Itsnaini, L.R., and Fitri, M.A., 2023, Synthesis and characterization of silica gel from Lapindo volcanic mud with ethanol as a cosolvent for desiccant applications, *RSC Adv.*, 13 (4), 2692–2699.

[52] Mahamuni, P.P., Patil, P.M., Dhanavade, M.J., Badiger, M.V., Shadija, P.G., Lokhande, A.C., and Bohara, R.A., 2019, Synthesis and characterization of zinc oxide nanoparticles by using polyol chemistry for their antimicrobial and antibiofilm activity, *Biochem. Biophys. Rep.*, 17, 71–80.

[53] Chieng, B.W., and Loo, Y.Y., 2012, Synthesis of ZnO nanoparticles by modified polyol method, *Mater. Lett.*, 73, 78–82.

[54] Qamar, O.A., Jamil, F., Hussain, M., Bae, S., Inayat, A., Shah, N.S., Waris, A., Akhter, P., Kwon, E.E., and Park, Y.K., 2023, Advances in synthesis of TiO_2 nanoparticles and their application to biodiesel production: A review, *Chem. Eng. J.*, 460, 141734.

[55] Zhang, W., Wang, C., Luo, B., He, P., Li, L., and Wu, G., 2023, Biodiesel production by transesterification of waste cooking oil in the presence of graphitic carbon nitride supported molybdenum catalyst, *Fuel*, 332 (Part 2), 126309.

[56] Zulfa, L.L., Ediati, R., Hidayat, A.R.P., Subagyo, R., Faaizatunnisa, N., Kusumawati, Y., Hartanto, D., Widiastuti, N., Utomo, W.P., and Santoso, M., 2023, Synergistic effect of modified pore and heterojunction of MOF-derived α-Fe_2O_3/ZnO for superior photocatalytic degradation of methylene blue, *RSC Adv.*, 13 (6), 3818–3834.